Proceedings of the 2021 Design of Medical Devices Conference
DMD2021
April 12-15, 2021, Minneapolis, MN, USA

DMD2021-1087

COMPUTATIONAL MODEL OF A TWO MATERIAL OBJECT PREDICTS NON-SYMMETRIC DISPERSAL VOLUME PROFILE

Brianna E. Morales
Department of Biomedical Engineering
The University of Texas at Austin
Austin, TX

Jason N. Mehta
Walker Department of Mechanical Engineering
The University of Texas at Austin
Austin, TX

Christopher G. Rylander
Walker Department of Mechanical Engineering
The University of Texas at Austin
Austin, TX

ABSTRACT

Convection-enhanced delivery (CED) is an experimental method of localized treatment to release high concentrations of the drug into a target area. An implementation of CED by our lab is the convection-enhanced thermo-therapy catheter system (CETCS). The device is a collection of arborizing microneedles used to affect a broader coverage of a dispersed volume in the regions of interest. We suspect the coverage of the dispersal volume depends on the material properties of the brain the infusate is being administered. In this study, we create a computational model to evaluate how two adjacent materials with varying permeability (4.45 $mm^4\ N^{-1}\ s^{-1}$ with 13.35 or 35.6 $mm^4\ N^{-1}\ s^{-1}$) will disperse into a 0.6% (w/w) agarose gel. Transient state analysis was conducted using the FEBio Software Suite. As expected, results show a much larger dispersal volume in the material with the higher permeability and along the border of the two materials.

Keywords: Convection-Enhanced Delivery, Computational Model, and Microneedles

NOMENCLATURE

c	Concentration
$\tilde{c}$	Effective concentration
D	Effective Diffusivity
D_o	Free Diffusivity
E	Elastic modulus
$\tilde{\kappa}$	Effective Solubility
k_o	Permeability
MW	Molecular Weight
θ	Temperature
ϕ	Osmotic coefficient
ρ	Density
φ^s	Solid volume fraction
$\tilde{p}$	Effective pressure,
p	Total pressure,
R	Universal gas constant
ν	Poisson's Ratio

1. INTRODUCTION

In the year 2020, there are expected to be less than 13,000 new cases of glioblastoma multiforme (GBM) in the US; however, the inability to effectively treat GBM leads to a high mortality rate with a survival time of about 12 to 18 months [1,2,4]. Current experimental treatments include convection-enhanced delivery (CED), which infuse a highly concentrated volume of drug to a target area within the brain via a pressure gradient. There have been many modifications to improve CED. Our lab has focused on a method that uses arborizing microneedles with fiber-optic light and drug delivery we call convection-enhanced thermo-therapy catheter system (CETCS) [7]. Previous work in our lab evaluated the benefit of the fiber optics and the evaluation of varying flow rates of infusate [5]. Additional work includes analyzing methods to improve the dispersed volume over the target area in a more realistic heterogeneous brain specific model.

1.1 Heterogeneous Brain Tumor Model

For GBM the target areas are the tumor itself and the tumor margins, areas surrounding the tumor. Recent work has identified high amounts of anisotropy in the white matter and nearly isotropic regions in the grey matter. The tumor comprises areas of high permeability, areas with neo vessels, and areas with necrotic cores. The fiber orientation may have a strong influence on the dispersed volume. Zhan et al. determined the effect of the anisotropic angle of the fibers in reference to the infusion catheter [8]. Nearly orthogonal oriented fibers had a horizontal dispersal profile, while fibers nearly aligned with the infusion cavity resulted in vertical dispersal profile. The complexity of the tissues in the tumor and the tumor margins can affect the dispersal profile.

2. MATERIALS AND METHODS

We conducted finite element analysis using FEBio Software Suite. The model was set up to evaluate the transient state of a

needle injecting into a single region of interest. This region of interest is heterogeneous, containing a material with a baseline permeability, 4.45 $mm^4\ N^{-1}\ s^{-1}$, and an adjacent material with higher permeability. We looked at two cases of varying the permeability by a factor of three and a factor of eight for this work.

2.1 The Geometry of the Model and the Model Environment

The model represents a region of interest within the brain in contact with a microneedle. We used a hollow sphere within a sphere to replicate the base geometry of the brain section in contact with a microneedle. To optimize the runtime of the experiment, we isolated half of the sphere and reduced it down to a single 3° slice, replicating a two-dimensional environment, as shown in **Figure 1**. The model environment was a biphasic-solute material. Isothermal conditions meant a constant model environment temperature of 298 K, room temperature. The 3° slice was separated into two materials, a baseline (Base) and the adjacent higher permeability (High). Since we are basing the material properties on a 0.6% (w/w) agarose gel, our base permeability is set to 4.45 $mm^4\ N^{-1}\ s^{-1}$ [6], while our high permeability is modified by a factor of three and eight to identify differences in the dispersal volume profile.

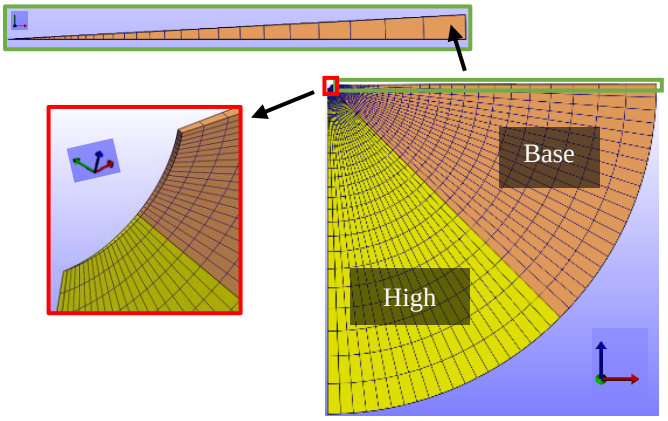

FIGURE 1: SIMPLIFIED 3D REPRESENTATION OF A CATHETER INJECTING INTO A SPHERICAL GEOMETRY. WITH ZOOMED IN AREAS OF THE UPPER REGION OF THE SLICE (GREEN BOX) AND THE INFUSION CAVITY (RED BOX)

2.2 Material properties

The material properties depend on the situation we would like to set up in our computational model. We prescribed material properties similar to the experimental setup we plan to do for 0.6% (w/w) agarose gel.

2.2.1 Indigo Carmine Dye

We modeled the infused drug as Indigo Carmine (IC) dye to follow previous experiments set up in our lab [6]. The material properties set for IC dye can be found in **Table 1.** These properties will be applied to a set of equations within the software and be used to represent the IC dye in the computational model.

Material Property	Value
Molecular Weight (MW)	$4.66E-06\ g\ nmol^{-1}$
Density (ρ)	$1.01E-03\ g\ mm^{-3}$
Free Diffusivity (D_0)	$6.0\ E-4\ mm^2\ s^{-1}$
Effective Diffusivity (D)	$5.5\ E-4\ mm^2\ s^{-1}$
Effective Solubility ($\tilde{\kappa}$)	1

TABLE 1: INDIGO CARMINE DYE MATERIAL PROPERTIES

2.2.2 Solid Matrix

The solid matrix properties were specific to the 0.6% (w/w) agarose gel. The values of data included in the model can be found in **Table 2.** Some values have been determined by previous work [3,5,6].

Material Property	Value
Solid volume fraction (φ^s)	0.006
Elastic Modulus (E)	6000 Pa
Poisson's Ratio (ν)	0.4
Permeability ($k0$)	4.45 $mm^4\ N^{-1}\ s^{-1}$

TABLE 2: SOLID MATRIX GEL MATERIAL PROPERTIES

2.3 Boundary Conditions and Applied Loads

To maintain equilibrium, we set the outside face to have a zero-fluid pressure. Besides the fluid pressure, we also set the displacement to be zero, to restrict motion, on several faces of the model. In **Figure 1**, the green box represents the top of the 3° slice, and the faces that make up this top region will be restricted in the z plane. Further referencing the green boxed area, the top portion of the triangular shape will act as a symmetry plane. The right side of the triangle is indicating the zero-fluid pressure, and on the bottom side, the point of the triangle represents the long side of the triangle and must be restricted in both the x and y planes.

2.3.1 Infusion Cavity

The infusion cavity represents the area in which the catheter encounters the brain model. For this area we have to set up equilibrium, using the equations below.

$$\tilde{c} = c/\tilde{\kappa} \qquad (1)$$

Where $\tilde{\kappa}$, is the effective solubility, is 1, making the ratio of the effective concentration, $\tilde{c}$, to the concentration, c, equal to 1. In our setup, we set $\tilde{c}$ to 0.001, and the computational solver outputs the concentration. We must set up the effective pressure on the cavity surface using the equation below.

$$\tilde{p} = p - R\theta\phi c \qquad (2)$$

Where we set the effective pressure, $\tilde{p}$, to 1300 Pa. Total pressure, p, is determined by the solver given the other variables in the equation: the universal gas constant, R, (8.315 $mm^3\ Pa\ K^{-1}\ nmol^{-1}$); temperature, θ, (298 K); the concentration; and the osmotic coefficient, ϕ, (set equal to 1).

In addition to the boundary conditions, we prescribe normal traction on the infusion surface equal to the negative of the prescribed effective pressure (-1300 Pa).

2.4 Transient State Analysis

Evaluation of the dispersal volume profile was performed over a time of 6000 s. We displayed the computational model at 100 minutes since we planned the experimental validation experiments to run for the same 100-minute duration.

3. RESULTS AND DISCUSSION

Figure 2 is the dispersal volume profile for the two cases of varying permeability by a factor of three (3X) and a factor of eight (8X). With a difference of a factor of three between the baseline and the higher permeability, the changes in the dispersal volume profile are subtle but apparent. In comparison, the difference of a factor of eight provides more contrasting dispersal volume profiles as expected. Dispersal in the high permeability region seems to provide additional dispersal into the base permeability region. Future iterations of this theoretical work should also include experimental work to determine if this leaking phenomenon is due to how the boundary conditions are set in the computational model, or if this is a true occurrence when two adjacent materials of varying permeabilities are being infused.

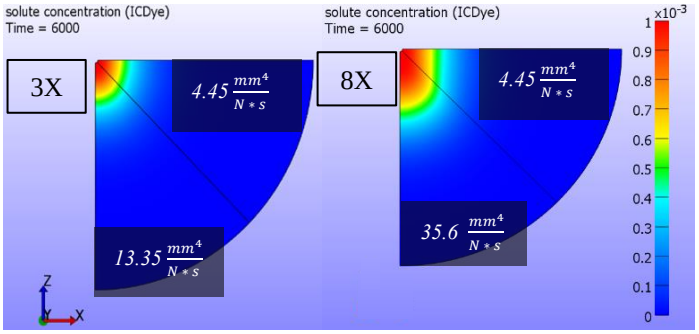

FIGURE 2: DISPERSAL VOLUME PROFILE OF THE IC DYE INTO A TWO MATERIAL OBJECT.

We determined the dispersal volume of the two cases, a factor of three (3X) and a factor of eight (8X), through post-processing of the data in MATLAB. The calculated dispersal volume was multiplied by 120° and doubled to reconstruct the full sphere from the single 3° slice model. When looking at the dispersal volume over 100 minutes it is clear, of the two dispersal volumes being compared in a single group, the base material ($M1_{3X}$ = 0.348 ml and $M1_{8X}$ = 0.613 ml) performs lower, regarding the profile of the V_d and the V_d, than the high material ($M2_{3X}$ = 0.966 ml and $M2_{8X}$ = 1.486 ml), as seen in **Figure 2** and **Figure 3**. Among the groups, there was a 177% increase from the base V_d to the high V_d for the 3X group, and a 142% increase from the base V_d to the high V_d for the 8X group. The total dispersal volumes for each group can be found in **Table 3**.

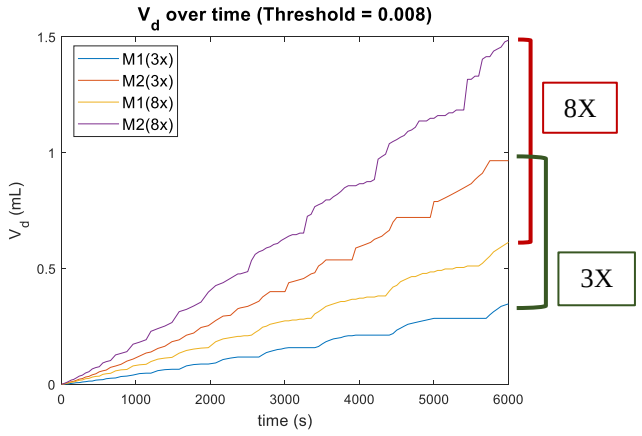

FIGURE 3: GRAPH OF THE V_d OVERTIME FOR A TWO MATERIAL OBJECT WHEN PERMEABILITIES, DIFFER BY A FACTOR OF THREE (3X) AND BY A FACTOR OF EIGHT (8X). OBJECT 1 (3X) HAS TWO MATERIAL TYPES, BASE (M1(3X)) AND HIGH (M2(3X)). OBJECT 2 (8X) HAS TWO MATERIAL TYPES, BASE (M1(8X)) AND HIGH (M2(8X)).

Group	Permeability	V_d (ml)
3X	Base - M1	0.348
	High - M2	0.966
8X	Base - M1	0.613
	High - M2	1.486

TABLE 3: TOTAL DISPERSAL VOLUME (V_d) FOR EACH MATERIAL

The ability to inform CETCS of a potential inhibitor to flow could allow quicker correction if the flow is too high in a region or if the dispersal volume is too large. For example, if the microneedle were to be inserted near the subarachnoid space or the ventricular system in the brain, the dispersal volume would be very large and result in a loss of highly concentrated drug into the CSF. However, if we know the signs of a significantly high permeability area, we could use the information to trigger the user of CETCS to correct the placement of the microneedles. The next steps for this research are to validate our theoretical data from the model with the experimental data of infusing IC dye

into a 0.6% (w/w) agarose gel, and to add layers of complexity to make the model more realistic such as introducing anisotropy into the model and more complex geometries.

3. CONCLUSION

This research highlights how two adjacent tissue types with unique material properties can affect the overall profile of the dispersal volume. It calls for a more dynamic and well-informed parameters to create a truly heterogeneous brain model to track the flow of drug into the brain caused by the CETCS device.

ACKNOWLEDGEMENTS

This research was funded by the National Institutes of Health/National Cancer Institute, grant number P01 CA207206-01.

REFERENCES

[1] Alexander, Brian M., and Timothy F. Cloughesy. *Journal of Clinical Oncology*, 2017.

[2] Cantrell, J. Nathan, Mark R Waddle, et al. *Mayo Clinic proceedings*, 2019.

[3] Chen, Xiaoming, and Malisa Sarntinoranont. *Annals of Biomedical Engineering*, 2007.

[4] Davis, Mary Elizabeth. *Clinical journal of oncology nursing*, 2016.

[5] Elenes, Egleide Yaneth. PhD diss., 2018.

[6] Elenes, E. Y., Rausch, M. K., and Rylander, C. G. *ASME J of Medical Diagnostics*, 2019.

[7] Hood, R. Lyle, Rudy T. Andriani Jr, Samantha Emch, John L. Robertson, Christopher G. Rylander, and John H. Rossmeisl Jr. *Lasers in surgery and medicine*, 2013.

[8] Zhan, Wenbo et al. *Drug delivery*, 2019.